

Uncertainty Quantification Metrics for Deep Regression

Ziliang Xiong^{*1}

Simon Kristoffersson Lind^{*2}

Per-Erik Forssén¹

Volker Krüger²

Abstract—When deploying deep neural networks on robots or other physical systems, the learned model should reliably quantify predictive uncertainty. A reliable uncertainty allows downstream modules to reason about the safety of its actions. In this work, we address metrics for evaluating such an uncertainty. Specifically, we focus on regression tasks, and investigate Area Under Sparsification Error (AUSE), Calibration Error, Spearman’s Rank Correlation, and Negative Log-Likelihood (NLL). Using synthetic regression datasets, we look into how those metrics behave under four typical types of uncertainty, their stability regarding the size of the test set, and reveal their strengths and weaknesses. Our results indicate that Calibration Error is the most stable and interpretable metric, but AUSE and NLL also have their respective use cases. We discourage the usage of Spearman’s Rank Correlation for evaluating uncertainties and recommend replacing it with AUSE.

I. INTRODUCTION

In recent years, there has been a rapid advance in the adoption of neural network-based methods for many tasks in robotics. Following this adoption, increasing scrutiny has been directed towards neural network-based methods for their lack of reliability and interpretability. While neural networks have achieved impressive performance for many different tasks, the fact remains that they can be unreliable in real-world deployment [1]. Additionally, their lack of interpretability makes it difficult to know how and when they may perform unreliably. For these reasons, increasing attention has been directed at the uncertainty output from neural networks, and the importance of introspective qualities [1]. Arguably the most important introspective quality is a reliable uncertainty estimate.

Despite increasing attention being directed toward *uncertainty quantification* (UQ), most of the work is directed toward uncertainty in classification tasks. In robotics, regression problems are common, and there is a lack of common understanding surrounding the available metrics. In this work, we have identified four metrics that are commonly used to measure various qualities in a predicted regression uncertainty. Specifically, we investigate the *Area Under Sparsification Error* (AUSE) [2], *Spearman’s Rank Correlation* [3], *Negative Log Likelihood* (NLL)[4], and *Calibration Error* [5]. These UQ metrics measure different aspects of uncertainty that are all orthogonal to the regression

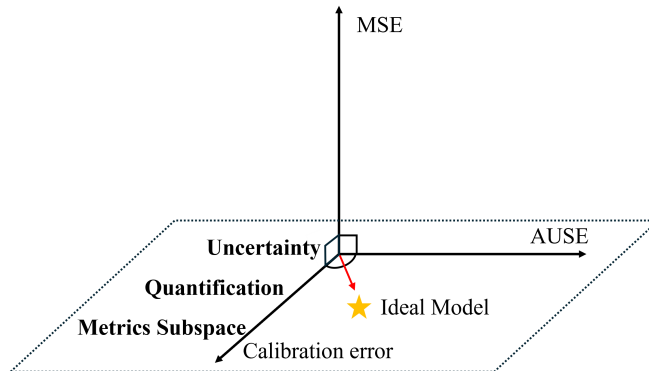


Fig. 1. An illustration for UQ metrics and regression metrics. Note: the axes of calibration error and AUSE are distinct, but not orthogonal.

task performance (typically *mean squared error* (MSE)) as indicated in Fig. 1.

With the help of synthetic datasets, we explore the usage of these metrics with the aim of understanding exactly what they measure, their limitations and whether or not their measurements are useful for practical applications.

Our contributions are as follows:

- We create simple synthetic datasets that highlight different types of uncertainty: 1) Homoscedastic aleatoric uncertainty; 2) Heteroscedastic aleatoric uncertainty; 3) Multimodal aleatoric uncertainty; 4) epistemic uncertainty.
- We compare each metric in terms of their stability to different dataset sizes.
- Using our datasets, we explore how different metrics behave under different types of uncertainty.
- We investigate how each metric behaves given the ground truth data distribution.
- Finally, we reason about the strengths and limitations of each metric.

As an additional contribution, we express a mathematical formulation for the AUSE metric. To the best of our knowledge, AUSE has previously only been described informally, using natural language.

II. RELATED WORK

Historically, methods that deal with any type of regression uncertainty have been formulated using parameterized distributions. Classic examples include Kalman filters [6], hidden Markov models [7], and Gaussian processes [8]. All of these employ parameterized distributions with well-defined measures of uncertainty. Modern machine learning methods are built upon a solid statistical foundation and most methods

* Equal contribution

¹ Dept. of EE, Linköping University, Linköping, Sweden
{firstname}.{lastname}@liu.se

² Dept. of CS, Lund University LTH, Lund, Sweden
{firstname}.{lastname}@cs.lth.se

This work has been submitted to the IEEE for possible publication. Copyright may be transferred without notice, after which this version may no longer be accessible.

output some form of uncertainty [9]. However, it has been observed that there is a discrepancy between the uncertainty output from modern neural networks, and the observed empirical accuracy [10]. Additionally, lacking interpretability in these uncertainties have led to the development of methods to formulate more statistically grounded uncertainties [11].

Along with the research on uncertainty estimation, a number of methods have been developed to assess how trustworthy a predicted uncertainty is. Perhaps the most commonly used (for example in [10], [12], [13], [14]) is the *expected calibration error* (ECE) [5]. While not as common as ECE, NLL (*negative log likelihood*) is also used, for example in [15], [16], [17]. Spearman’s rank correlation coefficient [3] has also found new use in this area (for example in [18], [19], [20]). Finally, the most recent method we examine is AUSE [2], used in for example [21], [22], [23]. While other uncertainty assessment methods exist, we have chosen to focus on these four as they are most commonly used.

III. THEORY

First, we introduce different types of uncertainty in Sec. III-A. Then, in Sec. III-B, we introduce the four common uncertainty evaluation metrics to be analyzed.

A. Different types of Uncertainty

In the realm of predictive uncertainty estimation, we encounter two fundamental types of uncertainty [24]. The first, known as *aleatoric uncertainty*, encompasses the intrinsic noise and ambiguity present in observations. This noise, stemming from sources like sensor or motion irregularities, persists even with an increase in data collection and cannot be mitigated. The second type, *epistemic uncertainty* constitutes the uncertainty surrounding model parameters, reflecting our lack of knowledge about the precise model generating the observed data. This form of uncertainty tends to diminish as more data is acquired, and is thus often termed *model uncertainty*. The most common cause of epistemic uncertainty is *out-of-distribution* (OOD) data. In other words, data that comes from a distribution that is different from the training data. For example, autonomous driving models that are trained on synthetic data usually face domain gap to real-world data.

Aleatoric uncertainty can be subdivided into *homoscedastic uncertainty*, which remains constant across various inputs, and *heteroscedastic uncertainty*, which varies depending on the model inputs. Heteroscedastic uncertainty plays a crucial role in computer vision tasks. For example, in depth regression, images with intricate textures and prominent vanishing lines typically yield confident predictions, whereas images of featureless surfaces are expected to result in significantly higher uncertainty.

B. Uncertainty Evaluation Metrics

Here, we introduce the four selected uncertainty metrics for the deep regression tasks. We define the metrics as functions of a dataset $S = \{(\mathbf{x}_i, y_i) \mid i = 1, 2, \dots, N\}$, consisting of input-output pairs (\mathbf{x}_i, y_i) .

For any learned model, we further define $F(\mathbf{x}; \theta) \mapsto \mathbb{R}$, and $U(\mathbf{x}; \theta) \mapsto \mathbb{R}$ to be functions based on the model parameters θ . $F(\mathbf{x}; \theta)$ produces a prediction of y , and $U(\mathbf{x}; \theta)$ produces an uncertainty estimate.

AUSE: Sparsification plots are widely used in optical flow [25], [26] and stereo disparity [27] to assess how well the predicted uncertainty coincides with the prediction error on a test dataset. Ilg et al.[2] define in natural language the numerical score AUSE for the comparison among approaches with different main task performances. Here we present a formal mathematical definition.

AUSE is computed as an aggregate metric over a dataset S consisting of input-output (\mathbf{x}_i, y_i) pairs. We define the *mean absolute error* (MAE) on S as:

$$\text{MAE}(S) = \frac{1}{|S|} \sum_{(\mathbf{x}_i, y_i) \in S} |y_i - F(\mathbf{x}_i; \theta)| . \quad (1)$$

Based on a parameter $\alpha \in [0, 1]$, we partition the set S into disjoint subsets $S_\wedge(\alpha)$ and $S_\vee(\alpha)$ such that $|S_\wedge(\alpha)| = \alpha|S|$, and

$$\begin{aligned} |y_i - F(\mathbf{x}_i; \theta)| &\geq |y_j - F(\mathbf{x}_j; \theta)| \\ \forall (\mathbf{x}_i, y_i) \in S_\wedge(\alpha), (\mathbf{x}_j, y_j) \in S_\vee(\alpha) . \end{aligned} \quad (2)$$

In other words, the size of $S_\wedge(\alpha)$ is a fraction α of the entire set S , and all absolute errors in $S_\wedge(\alpha)$ are larger than those in $S_\vee(\alpha)$. We also define analogous partitions $S_\wedge^U(\alpha)$ and $S_\vee^U(\alpha)$ with respect to the uncertainty:

$$\begin{aligned} U(\mathbf{x}_i; \theta) &\geq U(\mathbf{x}_j; \theta) \\ \forall (\mathbf{x}_i, y_i) \in S_\wedge^U(\alpha), (\mathbf{x}_j, y_j) \in S_\vee^U(\alpha) . \end{aligned} \quad (3)$$

With these partitions in place, we define the *area under sparsification error* (AUSE):

$$\begin{aligned} \text{AUSE}(S) &= \\ \frac{1}{\text{MAE}(S)} \int_0^1 &\text{MAE}(S_\vee^U(\alpha)) - \text{MAE}(S_\vee(\alpha)) d\alpha . \end{aligned} \quad (4)$$

AUSE computes the normalized area between the two curves $\text{MAE}(S_\vee^U(\alpha))$ and $\text{MAE}(S_\vee(\alpha))$ formed by varying α from 0 to 1. The curve $\text{MAE}(S_\vee(\alpha))$ is called the *oracle*, which represents a lower bound on the possible MAE of $S_\vee^U(\alpha)$. In practice, the integral in (III-B) is replaced with summing over $\alpha = [0, 1/N, \dots, 1]$ since the test set is finite. See Fig. 5 for an example.

Calibration Error The reliability diagram [28] and the *expected calibration error* (ECE) [5] are originally diagnostic tools for classification models that compare sample accuracy against predicted confidence. However, this approach does not apply to regression tasks. Therefore, Kuleshov et al. [12] introduce a calibration plot for regression tasks in terms of the cumulative distribution function from the model, and summarize it with *calibration error* as a numerical score. Formally, let the predicted probability distribution of an input

\mathbf{x}_i be $P_\theta^i = F(\mathbf{x}_i; \theta)$. We have the value of the predicted cumulative distribution function for the ground truth y_i as

$$P(y_i|\theta) = P_\theta^i(y \leq y_i|\theta). \quad (5)$$

The empirical frequency is then defined as

$$\hat{p}_j = \frac{|\{y_i \mid P(y_i|\theta) \leq p_j, (\mathbf{x}_i, y_i) \in S\}|}{N}. \quad (6)$$

Here $p_j \in [0, 1]$ represents an arbitrary threshold value. Given M distinct thresholds p_1, p_2, \dots, p_m (typically evenly spaced from 0 to 1), the calibration error is defined for regression as

$$\text{cal}(\hat{p}_1, \dots, \hat{p}_N) = \sum_{j=1}^M w_j (p_j - \hat{p}_j)^2, \quad (7)$$

where w_j are arbitrary scaling weights, usually $w_j = \frac{1}{N/\hat{p}_j}$.

Spearman correlation In 1904, psychologist Charles Spearman defined what he called the *rank method* of correlation [3]. He observed that there may exist correlations that would not be adequately captured by simple linear correlation. Instead, he argued that more complex correlations may be adequately captured by comparing *ranks* of elements.

Given a set of samples, the rank of a sample is simply the index that number would have in a list. More formally, let $L = [x_1, x_2, \dots, x_N]$ be a sequence of samples, then the rank of a sample is defined as:

$$r(x_i) = 1 + |\{x_j \mid x_j < x_i, x_j \in L\}|. \quad (8)$$

We then define the rank operation for a sequence:

$$R(L) = [r(x_1), r(x_2), \dots, r(x_N)]. \quad (9)$$

Spearman's rank method is then the correlation between two rank sequences:

$$\rho_{R(L_1), R(L_2)} = \frac{\text{cov}(R(L_1), R(L_2))}{\sigma_{R(L_1)} \sigma_{R(L_2)}}. \quad (10)$$

When used as a metric for uncertainty, this correlation is computed between the predictive uncertainty, and the absolute prediction errors.

NLL The popular negative log-likelihood is proved to be a *strictly proper scoring rule* [4]. Given a dataset $S = \{(\mathbf{x}_i, y_i) \mid i = 1, 2, \dots, N\}$ and a probability density function $p(y|\mathbf{x})$ parameterised by learnable parameters θ , the NLL is defined as

$$\text{NLL}(S) = -\sum_{i=1}^N \log p(y_i|\mathbf{x}_i; \theta). \quad (11)$$

In expectation, the NLL is minimized if and only if $p(y_i \mid \mathbf{x}_i; \theta)$ is equal to the true underlying data distribution [29]. As such, the NLL can also be used as a metric for uncertainty predictions, since a model with a lower NLL does a better job (in expectation) of fitting the true data distribution.

C. Regression Models with Uncertainty Predictions

There exist many different model architectures that incorporate uncertainty predictions. However, our goal is not to investigate properties in the models. We choose to only use two different models, namely an ensemble and an energy-based model.

1) *Deep Ensemble (DE)*: Ensemble learning combines the predictions from multiple individual models to achieve better predictive performance than any single model. For estimating predictive uncertainty, *Deep Ensemble* (DE) [4] is a simple yet effective method that trains multiple models in the same architecture with different random initialization and data shuffling. The ensemble is treated as a uniformly weighted mixture model. In practice, for the regression task, each individual model outputs two scalars, which are interpreted as the mean and variance of a Gaussian distribution, and then it is trained to minimize the Gaussian NLL loss as in (12) on the training set.

$$-\log p_\theta(y_n \mid \mathbf{x}_n) = \frac{\log \sigma_\theta^2(\mathbf{x})}{2} + \frac{(y - \mu_\theta(\mathbf{x}))^2}{2\sigma_\theta^2(\mathbf{x})} + C \quad (12)$$

We follow the suggestion in [4] to train 5 models and thus get a mixture of Gaussians. This mixture is further approximated by a Gaussian whose mean and variance are the mean and variance of the mixture respectively.

2) *Energy Based Regression (EBR)*: Energy-based learning involves learning an energy function $\mathcal{E}(x)$. The goal when learning $\mathcal{E}(x)$ is to assign low energy to observed samples [30]. Learning $\mathcal{E}(x)$ is in many ways analogous to learning a probability density function, and as such, it has commonly been used for unsupervised learning tasks [30]. Gustafsson *et al.* [30] construct a supervised regression model based on an energy function. First, they define $f_\theta(x, y) \mapsto \mathbb{R}$ to be their learned energy function. Then, they explicitly construct a probability density function:

$$p(y|x; \theta) = \frac{e^{f(x, y; \theta)}}{Z(x; \theta)}, \quad Z(x; \theta) = \int e^{f(x, \tilde{y}; \theta)} d\tilde{y}. \quad (13)$$

Parameters θ are trained by minimizing the NLL with respect to the training data:

$$\mathcal{L} = -\frac{1}{N} \sum_{i=1}^N \log Z(x_i; \theta) - f(x_i, y_i; \theta). \quad (14)$$

$Z(x_i; \theta)$ is approximated by Monte Carlo sampling. Predictions are generated by performing multi-start gradient ascent to maximize $f(x_i, \tilde{y}; \theta)$ with respect to \tilde{y} .

IV. EXPERIMENTS AND RESULTS

A. Synthetic Regression Datasets

In order to gauge the behavior of the different uncertainty metrics, we construct four simple synthetic regression datasets, each with a different source of uncertainty. These can be seen in Fig. 2. We will henceforth refer to these datasets by their names: *homoscedastic*, *heteroscedastic*, *multimodal*, and *epistemic*. The names, homoscedastic and

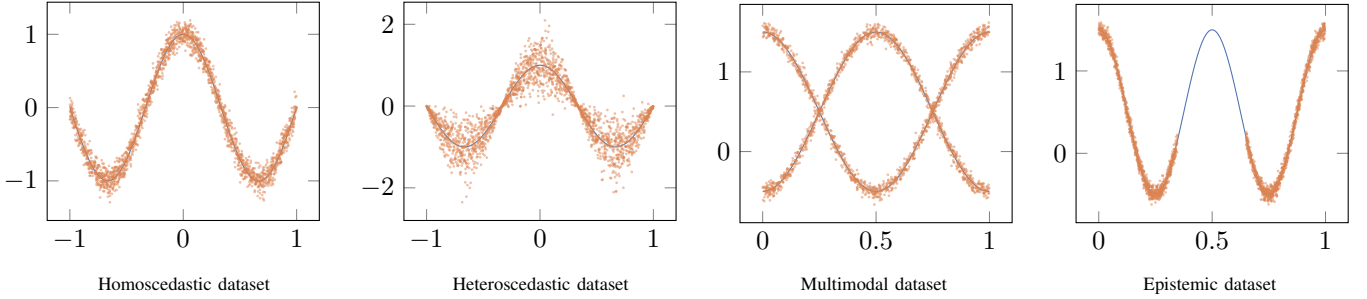


Fig. 2. The four synthetic regression datasets. Data points are orange, and the solid blue lines represent the expectation of the generating function.

heteroscedastic are in reference to the type of Gaussian noise applied to the generating function. Multimodal refers to the fact that data is generated from two separate generating functions. Finally, epistemic, refers to the epistemic uncertainty arising from a gap in the training data. Fundamentally, each dataset is a collection of input-output pairs (x, y) . Outputs y are generated as follows:

- Homoscedastic:

$$y = \cos(1.5\pi x) + \epsilon, \quad \epsilon \sim \mathcal{N}(0, 0.1) .$$
- Heteroscedastic:

$$y = \cos(1.5\pi x) + \epsilon, \quad \epsilon \sim \mathcal{N}(0, 0.4 \cdot |\cos(1.5\pi x)|) .$$
- Multimodal:

$$y = 0.5 \pm \cos(2\pi x) + \epsilon, \quad \epsilon \sim \mathcal{N}(0, 0.05) .$$
- Epistemic:

$$y = 0.5 + \cos(4\pi x) + \epsilon, \quad \epsilon \sim \mathcal{N}(0, 0.05) .$$

Here, $\mathcal{N}(0, \sigma)$ refers to a Gaussian distribution with mean 0, and standard deviation σ . When we write \pm in the definition of the multimodal dataset, we refer to a 50/50 chance of being + or -, which represents the two different modes. In the epistemic dataset, there is a gap in the training data for $x \in [0.35, 0.65]$, which is not present in the test data. This means test data is out of distribution, which causes epistemic uncertainty. Domains for the inputs are $x \in [-1, 1]$ for the homoscedastic and heteroscedastic datasets, and $x \in [0, 1]$ for the multimodal and epistemic datasets.

B. Implementation Details

For each synthetic dataset, we train one EBR model, and one DE model. Both types of models were trained with a batch size of 128 using the Adam [31] optimizer. Fig. 3 shows the resulting log-likelihood functions from the models, along with their predictions on our test sets.

Energy Based Regression Model We implement EBR model as a 9-layer perceptron with ReLU activations and a hidden size of 256, and we train for 20 epochs with a fixed learning rate of 10^{-4} .

Deep Ensemble All models in our ensemble are identical 5-layer perceptrons, with ReLU activations, and a hidden size of 256. We train each model in the ensemble for 20 epochs with a fixed learning rate of 10^{-3} . In our experiments we use the predicted variance as $U(x)$, more choices are compared in Xiong *et al.* [23].

C. Stability on varying test set sizes

All metrics require a test set for evaluation. Since a test set is, by necessity, a finite set of data points, each metric is an approximation. Therefore it is important to investigate how quickly each metric converges to its expected value. Additionally, each metric may be a biased approximation. We perform two experiments to test these two different aspects of stability.

First, in order to test convergence, we emulate a process of iteratively collecting points. We begin by generating a single large test dataset of size 2^{16} . From this dataset, we randomly sample data points without replacement, which allows us to investigate how the approximation of each metric behaves as the number of data points increases. We evaluate each metric at test set sizes $2^3, 2^4, \dots, 2^{16}$. The resulting metrics from each subset are reported in Fig. 4 (a).

Second, in order to investigate any bias in the approximation of each metric, we sample 100 i.i.d. datasets at each size $2^3, 2^4, \dots, 2^{16}$. We then report the average of each metric over these 100 datasets in Fig. 4 (b). If a metric is truly unbiased, the average at a small dataset size should converge to the same value as the average at larger dataset sizes.

For both of these experiments, we use our heteroscedastic dataset because we believe that it is the best candidate to highlight any stability issues, due to the varying noise levels present in the dataset.

D. Metrics under different types of uncertainty

For each dataset with different types of uncertainty, we compute all metrics for both our models on the test sets. Additionally, we wish to investigate how different metrics behave given the true data-generating distribution. Using the true data generating distribution will, in expectation, minimize NLL and calibration error, and should provide a good point of comparison for all metrics. We summarize metrics of both models for each dataset in Tab. I, II, III and IV respectively.

TABLE I
ALL METRICS FOR ALL MODELS ON HOMOSCEDASTIC DATASET.

	AUSE↓	Calibration Error↓	NLL↓
Ensemble	0.5915	0.0023	-0.8819
EBR	0.5707	0.0032	-0.8568
True dist.	0.5917	0.0003	-0.8965

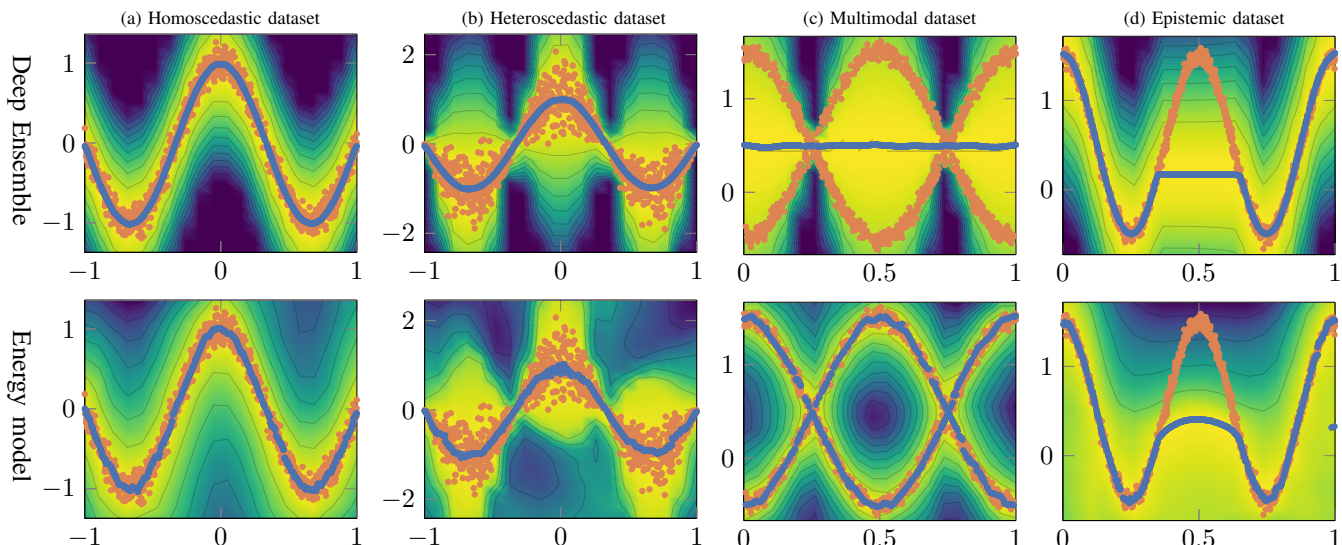


Fig. 3. Visualization of the predicted density on the test set for trained models. Contour plots: Log-likelihood output from each model. Yellow: the high-density region; Blue: the low-density region. Blue points: Predicted mean. Orange points: Ground truth.

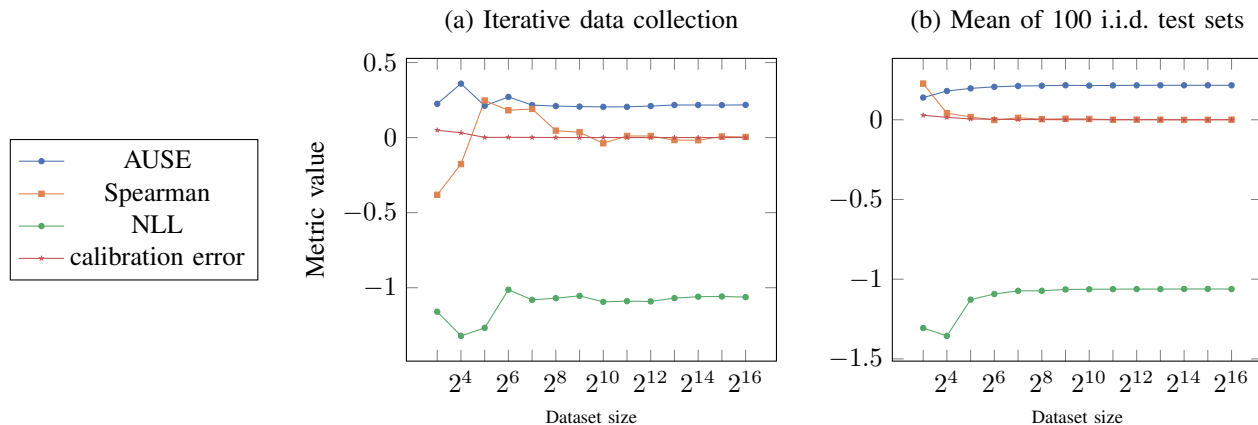


Fig. 4. Experiments to test two types of stability of metrics under different test dataset sizes.

TABLE II

METRICS FOR BOTH MODELS ON HETEROSCEDASTIC DATASET.

	AUSE↓	Calibration Error↓	NLL↓
Ensemble	0.2334	0.0001	-0.1091
EBR	0.2422	0.0001	-0.0990
True dist.	0.2305	0.0001	-0.1472

TABLE III

METRICS FOR BOTH MODELS ON MULTIMODAL DATASET.

	AUSE↓	Calibration Error↓	NLL↓
Ensemble	0.0071	0.0229	0.8098
EBR	0.5821	0.0018	-0.6535
True dist.	0.5180	0.0001	-0.7935

TABLE IV

METRICS FOR BOTH MODELS ON EPISTEMIC DATASET.

	AUSE↓	Calibration Error↓	NLL↓
Ensemble	0.6016	0.0145	36.4332
EBR	1.3888	0.0298	31.2425
True dist.	0.5454	0.0001	-1.5871

V. DISCUSSION

Here we analyze the experiment results, and reason about various strengths and limitations of each metric.

A. Stability on varying test set sizes

From Fig. 4 (a) we can see that all metrics vary as the test set sizes increase and finally converge to the expectation. We can conclude that all metrics converge beyond a dataset size of 2^{10} ($=1024$). Hence, for most modern regression applications, where test datasets are larger than ~ 1000 samples, stability should not be a cause for concern. Though the amplitudes of metrics vary from each other, arguably we can also conclude that **calibration error is the most stable and AUSE converges second fastest**.

From Fig. 4 (b) we can see that the averages change for different dataset sizes. We will henceforth refer to this behavior as *estimation bias of mean*. Arguably, estimation bias is undesirable, since we expect the average of a metric to converge to the same value regardless of the dataset size. As such, a metric with significant bias of the mean should be considered unstable and its use discouraged. Overall,

calibration error is the most stable and AUSE the second most in terms of bias of the mean. We can also conclude that no metric seems to exhibit any meaningful bias beyond a dataset size of 2^6 . On the other hand, there is still visible bias with dataset size 2^5 , where the total number of samples collected in 100 test sets is much larger than the previously suggested size 2^{10} . This indicates that it is advantageous to collect one large test set compared to aggregating many smaller test sets.

Together, these two plots suggest that **the most stable metric is calibration error, followed by AUSE, then NLL, and finally Spearman correlation.** Surprisingly, in both Fig. 4 (a) and (b), Spearman correlation has a large value with small test set sizes and gradually converges to zero as the test set size grows. This can be explained by a closer look at Fig. 3 (b): All points close to $x = 0$ will have similar predicted uncertainty values, but their errors may be vastly different, which counteracts the correlation between error and uncertainty. Naturally, this counteracting effect becomes less impactful when samples are sparse. By extension, it is also less impactful in higher-dimensional spaces, and Spearman correlation has been used successfully on for example the rMD17 dataset [32].

B. Metrics under different types of uncertainty

Results for Spearman correlation will not be displayed in the following experiments as it converges to zero.

Homoscedastic and Heteroscedastic datasets: we first look at the predicted density distribution in Fig. 3 (a) and (b) for each model. We can see that both models learn distributions close to the generating functions (see Sec. IV-A) for both datasets.

In Tab. I and II, all metrics suggest that both models learn the homoscedastic and heteroscedastic distributions approximately equally well. Interestingly, AUSE seems to imply that the EBR model has learned a distribution that is better than the ground truth of the homoscedastic dataset. Looking at Fig. 5 (a), the sparsification curve is nearly horizontal, because the predicted variances are nearly uniform over the entire test set. It is hence impossible to learn a meaningful correlation between errors and uncertainty. The predicted variance can only partially explain the error, the remaining part is caused by the difference between the annotation and the predicted mean. Intuitively, we expect this scenario of a perfectly uniform variance to be rare in real-world applications. This also indicates that generating uncertainty measures from the predicted distribution may not be the optimal approach for sorting samples based on uncertainty. For the heteroscedastic dataset, the true distribution achieves the best NLL, and the DE model is slightly better than EBR model. This is because the DE model learns a sharper distribution than EBR, as can be seen in the contour plots of Fig. 3 (a). NLL, being a proper scoring rule, addresses calibration and sharpness simultaneously [33].

Multimodal dataset: we first look at the predicted density distribution in Fig. 3 (c) for each model. The energy-based model successfully learns both modes. Our ensemble

was never designed to output multimodal predictions, and therefore it entirely fails to capture the multimodality.

Tab. III shows larger discrepancy between metrics. All metrics suggest that the energy-based model has learned a good distribution that is close to the ground truth distribution. AUSE seems to imply that the DE model has learned a near-perfect uncertainty predictor, even significantly better than the ground truth. Calibration error and NLL both successfully reflect the ensemble’s failure to learn both modes. This highlights the main difference between AUSE (and Spearman correlation) and calibration error/NLL: AUSE measures a correlation between uncertainty and the absolute error, while calibration error and NLL measure how well the learned distribution captures the data. Naturally, this raises the question of which type of measurement is most useful, which we will discuss in Sec. V-D.

Epistemic dataset: In Fig. 3 (d), both models exhibit somewhat larger uncertainty in the OOD region. However, neither model predicts a distribution that assigns high probability to the test data. Visually, the predicted distributions of both models look extremely similar. The only obvious perceptible difference is the slight bend in the center of the distribution of the EBR model.

In Tab. IV, AUSE seems to imply that the ensemble has learned a distribution that is almost as good as the ground truth, while it says the EBR model failed spectacularly. Both calibration error and NLL agree that both models failed to learn a good distribution, but they disagree on which model is worse. The contours in Fig. 3 (d) also shows the DE model gives sharper distribution. It is worth noting that there is an entire field of study of Out-of-Distribution detection, which offers better methods for handling epistemic uncertainty. Hence, we are only interested in whether or not each metric can capture our models’ failure to learn the underlying distribution.

Looking at the AUSE scores of 0.6016 and 1.3888 for the ensemble and EBR models respectively, we can infer that this small bend reduces the correlation between error and uncertainty enough to (more than) double the AUSE score. Intuitively, we would expect these two similar distributions to get similar scores, which is exactly the case with both calibration error and NLL. This raises questions regarding the stability of AUSE under small model variations.

C. Interpretability

Finally, an important aspect of metrics is their interpretability. Calibration error reaches the lower bound 0 when the predicted distributions are close to the ground truth. The upper bound 1 is when all the test samples have nearly zero values of cumulative density. While calibration error is highly interpretable, the same cannot be said for NLL and AUSE. With NLL and AUSE, we can compare UQ across models, however, the lower and upper bounds are unclear.

NLL: The lower bound of NLL is given by the ground truth distribution. But when training for real-world deployment, the true data distribution is typically unknown. The upper bound is positive infinity.

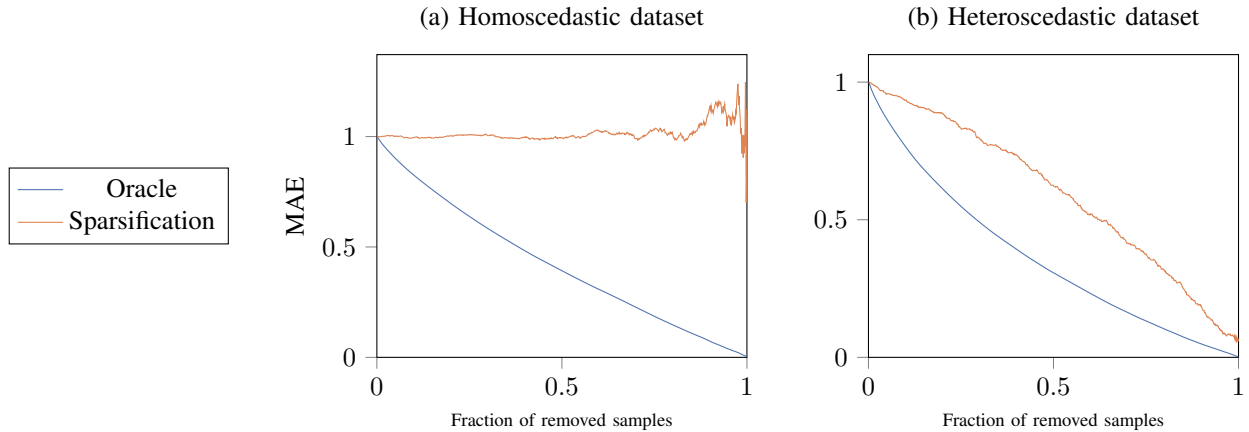


Fig. 5. Sparsification plots from Deep Ensemble, for the Homoscedastic and heteroscedastic datasets.

AUSE: From Sec. V-B we know that ground truth distribution may not even give the optimal lower bound 0. We argue that predicted variance can only partially explain the error. There is no clear upper bound for AUSE.

To sum up, there is no reference frame for the magnitudes of NLL and AUSE if ground truth distributions are unknown. I.E., NLL and AUSE can only tell us which model is better at UQ but cannot tell us how good it is. Hence, the lack of interpretability consists of a severe limitation of applying AUSE and NLL into real-world autonomous systems.

D. Strengths and Limitations

AUSE

- **Strengths:** It offers a robust quantized measure on the correlation between predictive uncertainty and errors compared with Pearson correlation and Spearman correlation. It tells how wrong a model’s prediction is likely to be, which is vital for trust-worthy autonomous system. It is more appropriate for loss prediction [34], [35], which is another UQ approach compared to predicting full distributions.
- **Limitations:** The value is not bounded thus, lacks interpretability; It may fail in tasks where homoscedastic uncertainty is dominant, which is rare in real-world applications; It does not comply with distribution prediction approach since the generating distribution does not return optimal AUSE.

Calibration Error

- **Strengths:** The value is statistically bounded and thus interpretable; It requires the least amount of samples to be stable, and is thus less demanding for collecting test data; The definition is flexible to extend to general confidence intervals beyond the cumulative distribution.
- **Limitations:** It requires predicting a distribution; It does not capture how wrong the predictions can be.

NLL

- **Strengths:** It measures the shape of the predictive distributions, including calibration and sharpness.
- **Limitations:** It fails when the ground truth distribution is multimodal but the training target is unimodal[23];

It requires largest amount of test samples to be stable compared with the other two metrics.

Spearman Correlation Limitations are covered in Sec. V-A.

E. Concluding Remarks

Essentially calibration error and NLL measure how well the predicted probability distribution corresponds to the true data generating distribution, whereas AUSE and Spearman measure how well the predicted uncertainty can tell the magnitude of errors. Which approach is deemed most useful will naturally differ between applications. For example, if an autonomous car is driving towards a wall, it needs to steer either left or right, but the exact turning angle is less important. In such a scenario the EBR model is clearly a better choice, and calibration error or NLL are clearly more appropriate metrics. On the other hand, in a scenario where an autonomous car has to follow a road in poor visibility, then it is likely better to keep straight and report a high uncertainty, in which case the ensemble is the better model, and AUSE is the better metric.

In conclusion, we have tested four common uncertainty assessment metrics on four synthetic datasets that are designed to illustrate properties of these metrics. Calibration error and NLL exhibit similar properties, but calibration error is the more interpretable of the two. AUSE and Spearman correlation seem more appropriate for models that predict the loss directly instead of predicting the distribution. In our experiments AUSE has consistently proved to be more robust than Spearman, and therefore we discourage the use of Spearman correlation for uncertainty quantification.

Acknowledgement: This work was funded by Swedish national strategic research environment ELLIIT, grant C08. Computational resources were provided by the National Academic Infrastructure for Supercomputing in Sweden (NAISS).

REFERENCES

- [1] H. Grimmert, R. Triebel, R. Paul, and I. Posner, “Introspective classification for robot perception,” *The International Journal of Robotics Research*, vol. 35, no. 7, p. 743–762, June 2016.

- [2] E. Ilg, O. Cicek, S. Galesso, A. Klein, O. Makansi, F. Hutter, and T. Brox, "Uncertainty estimates and multi-hypotheses networks for optical flow," in *Proceedings of the European Conference on Computer Vision (ECCV)*, 2018, pp. 652–667.
- [3] C. Spearman, "The proof and measurement of association between two things," *The American Journal of Psychology*, vol. 15, no. 1, p. 72–101, 1904.
- [4] B. Lakshminarayanan, A. Pritzel, and C. Blundell, "Simple and scalable predictive uncertainty estimation using deep ensembles," *Advances in neural information processing systems*, vol. 30, 2017.
- [5] M. Pakdaman Naeini, G. Cooper, and M. Hauskrecht, "Obtaining well calibrated probabilities using bayesian binning," *Proceedings of the AAAI Conference on Artificial Intelligence*, vol. 29, no. 1, Feb. 2015. [Online]. Available: <https://ojs.aaai.org/index.php/AAAI/article/view/9602>
- [6] R. E. Kalman, "A new approach to linear filtering and prediction problems," *Transactions of the ASME—Journal of Basic Engineering*, vol. 82, no. Series D, pp. 35–45, 1960.
- [7] A. van den Bosch, *Hidden Markov Models*. Boston, MA: Springer US, 2017, p. 609–611. [Online]. Available: https://doi.org/10.1007/978-1-4899-7687-1_124
- [8] C. E. Rasmussen and C. K. I. Williams, *Gaussian Processes for Machine Learning*. The MIT Press, Nov. 2005. [Online]. Available: <https://direct.mit.edu/books/book/2320/Gaussian-Processes-for-Machine-Learning>
- [9] C. M. Bishop, *Pattern recognition and machine learning*, ser. Information science and statistics. New York: Springer, 2006.
- [10] C. Guo, G. Pleiss, Y. Sun, and K. Q. Weinberger, "On calibration of modern neural networks," in *International conference on machine learning*. PMLR, 2017, pp. 1321–1330.
- [11] J. Gawlikowski, C. Rovile Njéutcheu Tassi, M. Ali, J. Lee, M. Humt, J. Feng, A. Kruspe, R. Triebel, P. Jung, R. Roscher, M. Shahzad, W. Yang, R. Bamler, and X. X. Zhu, "A Survey of Uncertainty in Deep Neural Networks," *Artificial Intelligence Review*, vol. 56, pp. 1513–1589, July 2023.
- [12] V. Kuleshov, N. Fenner, and S. Ermon, "Accurate uncertainties for deep learning using calibrated regression," in *Proceedings of the 35th International Conference on Machine Learning*. PMLR, July 2018, p. 2796–2804. [Online]. Available: <https://proceedings.mlr.press/v80/kuleshov18a.html>
- [13] S. Thulasidasan, G. Chennupati, J. A. Bilmes, T. Bhattacharya, and S. Michalak, "On mixup training: Improved calibration and predictive uncertainty for deep neural networks," in *Advances in Neural Information Processing Systems*, H. Wallach, H. Larochelle, A. Beygelzimer, F. d. Alché-Buc, E. Fox, and R. Garnett, Eds., vol. 32. Curran Associates, Inc., 2019.
- [14] M. Minderer, J. Djolonga, R. Romijnders, F. Hubis, X. Zhai, N. Houlsby, D. Tran, and M. Lucic, "Revisiting the calibration of modern neural networks," in *Advances in Neural Information Processing Systems*, vol. 34. Curran Associates, Inc., 2021, p. 15682–15694.
- [15] J. Heiss, J. Weissteiner, H. Wutte, S. Seuken, and J. Teichmann, "NOMU: Neural optimization-based model uncertainty," in *Proceedings of the 39th International Conference on Machine Learning*, no. PLMR 162, 2022.
- [16] A. Loquercio, M. Segu, and D. Scaramuzza, "A general framework for uncertainty estimation in deep learning," *IEEE Robotics and Automation Letters*, vol. 5, no. 2, p. 3153–3160, Apr. 2020.
- [17] T. Pearce, F. Leibfried, A. Brintrup, M. Zaki, and A. Neely, "Uncertainty in neural networks: Approximately bayesian ensembling," in *Proceedings of the 23rd International Conference on Artificial Intelligence and Statistics (AISTATS)*, no. PMLR vol. 108, 2020.
- [18] A. R. Tan, S. Urata, S. Goldman, J. C. B. Dietschreit, and R. Gómez-Bombarelli, "Single-model uncertainty quantification in neural network potentials does not consistently outperform model ensembles," *npj Computational Materials*, vol. 9, no. 1, p. 1–11, Dec. 2023.
- [19] M. Ng, F. Guo, L. Biswas, S. E. Petersen, S. K. Piechnik, S. Neubauer, and G. Wright, "Estimating uncertainty in neural networks for cardiac mri segmentation: A benchmark study," *IEEE Transactions on Biomedical Engineering*, vol. 70, no. 6, p. 1955–1966, June 2023.
- [20] X. Qiu, E. Meyerson, and R. Miikkulainen, "Quantifying point-prediction uncertainty in neural networks via residual estimation with an *i/o* kernel," in *In proceedings of International Conference on Learning Representations (ICLR)*, 2020. [Online]. Available: <https://openreview.net/pdf?id=rkxNh1Stvr>
- [21] A. Eldesokey, M. Felsberg, K. Holmquist, and M. Persson, "Uncertainty-aware cnns for depth completion: Uncertainty from beginning to end," in *Proceedings of the IEEE/CVF Conference on Computer Vision and Pattern Recognition (CVPR)*, June 2020.
- [22] C. Wang, X. Wang, J. Zhang, L. Zhang, X. Bai, X. Ning, J. Zhou, and E. Hancock, "Uncertainty estimation for stereo matching based on evidential deep learning," *Pattern Recognition*, vol. 124, p. 108498, Apr. 2022.
- [23] Z. Xiong, A. Eldesokey, J. Johnander, B. Wandt, and P.-E. Forssén, "Hinge-wasserstein: Mitigating overconfidence in regression by classification," in *IEEE Computer Society Conference on Computer Vision and Pattern Recognition Workshops (CVPRW 2024)*, 2024.
- [24] A. Kendall and Y. Gal, "What uncertainties do we need in bayesian deep learning for computer vision?" *Advances in neural information processing systems*, vol. 30, 2017.
- [25] O. Mac Aodha, A. Humayun, M. Pollefeys, and G. J. Brostow, "Learning a confidence measure for optical flow," *IEEE Transactions on Pattern Analysis and Machine Intelligence*, vol. 35, no. 5, pp. 1107–1120, 2013.
- [26] A. S. Wannenwetsch, M. Keuper, and S. Roth, "Probflow: Joint optical flow and uncertainty estimation," in *2017 IEEE International Conference on Computer Vision (ICCV)*, 2017, pp. 1182–1191.
- [27] G. Häger, M. Persson, and M. Felsberg, "Predicting disparity distributions," in *2021 IEEE International Conference on Robotics and Automation (ICRA)*, 2021, pp. 4363–4369.
- [28] A. Niculescu-Mizil and R. Caruana, "Predicting good probabilities with supervised learning," in *Proceedings of the 22nd international conference on Machine learning*, ser. ICML '05. New York, NY, USA: Association for Computing Machinery, Aug. 2005, p. 625–632. [Online]. Available: <https://doi.org/10.1145/1102351.1102430>
- [29] T. Hastie, R. Tibshirani, and J. Friedman, *The Elements of Statistical Learning*, ser. Springer Series in Statistics. New York, NY: Springer, 2009. [Online]. Available: <http://link.springer.com/10.1007/978-0-387-84858-7>
- [30] F. K. Gustafsson, M. Danelljan, G. Bhat, and T. B. Schön, "DCTD: deep conditional target densities for accurate regression," *CoRR*, vol. abs/1909.12297, 2019. [Online]. Available: <http://arxiv.org/abs/1909.12297>
- [31] D. Kingma and J. Ba, "Adam: A method for stochastic optimization," in *International Conference on Learning Representations (ICLR)*, San Diego, CA, USA, 2015.
- [32] A. Christensen, Anders S.; Von Lilienfeld, "Revised md17 dataset (rmd17)." <https://doi.org/10.6084/m9.figshare.12672038.v3>. 2020.
- [33] T. Gneiting and A. E. Raftery, "Strictly proper scoring rules, prediction, and estimation," *Journal of the American statistical Association*, vol. 102, no. 477, pp. 359–378, 2007.
- [34] D. Yoo and I. S. Kweon, "Learning loss for active learning," in *2019 IEEE/CVF Conference on Computer Vision and Pattern Recognition (CVPR)*, 2019, pp. 93–102.
- [35] P. Cui, D. Zhang, Z. Deng, Y. Dong, and J. Zhu, "Learning sample difficulty from pre-trained models for reliable prediction," *Advances in Neural Information Processing Systems*, vol. 36, 2024.